**doi: 10.12029/gc20200709002**

吴浩,徐祖阳,严维兵,郝宇杰,刘海永. 2023. 西藏中部聂尔错地区辉绿岩锆石U-Pb年龄与地球化学特征:对新特提斯洋板片断离的指示[J]. 中国地质, 50(6): 1804-1816.

Wu Hao, Xu Zuyang, Yan Weibing, Hao Yujie, Liu Haiyong. 2023. Zircon U-Pb ages and geochemical characteristics of diabase in Nie'erco area, central Tibet: Implication for Neo-Tethyan slab breakoff[J]. Geology in China, 50(6): 1804-1816(in Chinese with English abstract).

# 西藏中部聂尔错地区辉绿岩锆石U-Pb年龄与地球化学特征:对新特提斯洋板片断离的指示

吴浩[1,2],徐祖阳[3],严维兵[3],郝宇杰[4],刘海永[5]

(1. 桂林理工大学地球科学学院,广西 桂林 541004;2. 河海大学地球科学与工程学院,江苏 南京 211100;3. 江苏省地质勘查技术院,江苏 南京 210000;4. 自然资源部东北亚矿产资源评价重点实验室,吉林 长春 130061;5. 西藏自治区地质调查院,西藏 拉萨 850000)

**提要:【研究目的】**幔源岩浆活动是探讨深部动力学演化的理想研究对象,西藏中部聂尔错地区广泛发育的基性岩脉无疑是探讨区域构造-岩浆演化的关键所在。**【研究方法】**本文对聂尔错辉绿岩脉进行了系统的岩石学、地质年代学和地球化学综合研究。**【研究结果】**分析结果表明,聂尔错辉绿岩锆石U-Pb定年结果为(50.8±0.6)Ma,为始新世早期岩浆活动的产物。全岩地球化学组成显示辉绿岩具有低$SiO_2$、高MgO、$Al_2O_3$、$TiO_2$和全碱含量($Na_2O+K_2O$),富集轻稀土元素、亏损重稀土元素等特征,显示碱性洋岛型玄武岩(OIB)的地球化学特征。地球化学特征指示辉绿岩可能起源于软流圈地幔,同时岩浆在上升过程中受到一定程度的地壳物质混染。**【结论】**结合西藏南部地区广泛发育的同时期碰撞后林子宗火山岩与OIB型基性岩,研究认为西藏地区新生代岩浆活动主要受控于新特提斯洋的北向俯冲以及印度-欧亚板块的碰撞过程,板片断离所导致的上涌软流圈地幔减压熔融是聂尔错辉绿岩最为合理的成因解释。

**关 键 词:**锆石U-Pb年龄;辉绿岩;始新世;新特提斯洋;板片断离;地质调查工程;聂尔错;西藏

**创 新 点:**(1)聂尔错辉绿岩形成于始新世(51 Ma),具有OIB型岩石的地球化学特征;(2)聂尔错OIB型辉绿岩的识别为新特提斯洋闭合后板片断离提供了重要的证据。

**中图分类号:** P581;P597;P541 **文献标志码:** A **文章编号:** 1000-3657(2023)06-1804-13

# Zircon U-Pb ages and geochemical characteristics of diabase in Nie'erco area, central Tibet: Implication for Neo-Tethyan slab breakoff

WU Hao[1,2], XU Zuyang[3], YAN Weibing[3], HAO Yujie[4], LIU Haiyong[5]

(1. *College of Earth Sciences, Guilin University of Technology, Guilin* 541004*, Guangxi, China;* 2. *School of Earth Sciences and Engineering, Hohai University, Nanjing* 211100*, Jiangsu, China;* 3. *Geological Exploration Technology Institute of Jiangsu Province, Nanjing* 210000*, Jiangsu, China;* 4. *Key Laboratory of Mineral Resources Evaluation in Northeast Asia, Ministry of Natural Resources of China, Changchun* 130061*, Jilin, China;* 5. *Tibet Institute of Geological Survey, Lhasa* 850000*, Tibet, China*)

**收稿日期:**2020-07-09;**改回日期:**2020-08-25

**基金项目:**江苏省基础研究计划(自然科学基金)资助项目(BK20170877)资助。

**作者简介:**吴浩,男,1989年生,副教授,主要从事岩石大地构造研究;E-mail:wuhaojlu@126.com。

**Abstract:** This paper is the result of geological survey engineering.

**[Objective]** Mantle-derived magmatism generally provided an ideal research object to reveal the geodynamic evolution in the depth. The mafic dikes, which shown intensive distribution in Nie'erco area of central Tibet, are regarded as a key aspect to understanding the regional tectono-magmatic evolution. **[Methods]** In this paper, we report geochronological and geochemical data of the diabases in the Nie'erco area. **[Results]** The zircon U-Pb dating yielded magmatic crystallization ages of (50.8±0.6) Ma, indicating the Nie'erco diabases emplacement in the early Eocene. The diabase samples have low $SiO_2$, high MgO, $Al_2O_3$, $TiO_2$ and total alkali ($Na_2O+K_2O$) contents, similar to alkaline ocean island basalt (OIB). These geochemical features suggest that the studied diabases were generated by partial melting of asthenosphere, with the involvement of continental crustal components. **[Conclusions]** Combined with the post-collisional Linzizong volcanic rocks and OIB-like mafic rocks in southern Tibet, we prefer that the Cenozoic magmatism in Tibet is mainly controlled by the northward subduction of the Neo-Tethyan ocean and the following continent collision between India and Eurasia plates. Our research favor that the Nie'erco diabases were generated in response to the slab breakoff and related upwelling and decompressional melting of sub-slab asthenosphere.

**Key words:** zircon U-Pb age; diabase; Eocene; Neo-Tethys; slab breakoff; geological survey engineering; Nie'erco; Tibet

**Highlights:** (1) Nie'erco diabases emplaced in Eocene (51 Ma) and shown geochemical affinity to OIB-type rocks; (2) Identification of OIB-like diabases provided important evidence for the slab breakoff of Neo-Tethyan Ocean.

**About the first author:** WU Hao, male, born in 1989, associate professor, mainly engaged in petrochemistry and geotectonics; E-mail: wuhaojlu@126.com.

**Fund support:** Supported by Natural Science Foundation of Jiangsu Province (No.BK20170877).

## 1　引　言

印度—欧亚板块之间的碰撞是新生代以来最具全球性意义的地质事件，它直接导致了喜马拉雅造山带的形成以及青藏高原的快速抬升，并伴随有强烈的构造-岩浆-变质-成矿作用（潘桂棠等，2006；侯增谦等, 2006；莫宣学，2011；许志琴等，2011，2016；任继舜等, 2017；赵亚云等，2022）。受新特提斯洋闭合以及印度-欧亚板块陆陆碰撞过程的影响，在拉萨地块的南缘爆发了大规模的岩浆作用，这些岩浆岩为示踪岩浆源区物质组成、探讨造山带深部大陆动力学过程提供了理想的研究对象（Chung et al., 2003；赵志丹等，2006；莫宣学，2011；孟元库等，2015，2018；汪斌等，2022）。

研究表明始新世是新特提斯洋消亡后、印度-欧亚板块之间陆陆碰撞的初始期，拉萨地块南缘大规模发育的林子宗群以及同时期侵入岩被认为是该事件最为直接的岩浆记录，国内外学者已经对该期岩浆作用进行了大量的研究工作，在岩浆岩时空格架、岩石成因、深部动力学机制等方面取得了重要的进展（Chung et al., 2003, 2005；赵志丹等，2006；Zhu et al., 2015，2018）。然而以往的研究工作主要集中在岩浆岩发育的拉萨地块南缘，而在远离印度-欧亚板块碰撞带的西藏中部地区，始新世岩浆活动弱，研究程度较低。近年来，西藏中部局部地区陆续报道了始新世岩浆岩资料，但是这些岩浆岩以中酸性岩石为主，难以准确约束成岩构造背景，不同学者对该期岩浆作用的深部动力学机制仍存在不同的认识，部分学者认为是新特提斯洋北向俯冲板片断离机制下的岩浆产物，而也有部分学者则认为是印度-欧亚板块碰撞导致班公湖—怒江缝合带再次活动的产物（付文春等，2014；魏永峰等，2018；张耀玲等，2018）。可以看出，西藏中部始新世岩浆活动的深部动力学机制仍存有争议，其与南侧大规模发育的同时期岩浆作用之间的成因联系尚不明确，亟待进一步研究。

本文对西藏中部聂尔错地区新识别的辉绿岩脉进行了锆石U-Pb测年与全岩地球化学研究工作，以此查明辉绿岩的形成时代与岩石成因，进一步探讨成岩深部动力学机制、约束印度-欧亚板块之间的汇聚过程。

## 2　地质概况与岩石学特征

青藏高原经历了不同时期特提斯洋多期次开合以及板块汇聚过程，形成了近东西向展布的多个构造缝合带，这些缝合带从南至北依次将青藏高原

划分为喜马拉雅、拉萨、羌塘、松潘甘孜和祁连—昆仑等地块(Yin and Harrison, 2000; 潘桂堂等, 2006; 许志琴等, 2011; 任纪舜等, 2017)。其中拉萨地块南侧以雅鲁藏布缝合带为界,北侧以班公湖—怒江缝合带为界,其内部又以米拉山断裂和狮泉河—永珠—嘉黎缝合带进一步划分为南、中、北三个次级地块(图1)(Zhu et al., 2011)。

受南侧新特提斯洋北向俯冲以及印度-欧亚板块碰撞过程的影响,在中南拉萨地块上广泛发育着的中—新生代的弧型岩浆活动(Chung et al., 2003, 2005; 莫宣学, 2011; Zhu et al., 2015, 2018; 孟元库等, 2018);而北拉萨地块上岩浆岩主要形成于中生代晚期,一般认为是班公湖—怒江洋俯冲消减以及拉萨—羌塘板块碰撞等构造演化过程的记录(Zhu et al., 2011; Wu et al., 2019a, b; Yu et al., 2022;吴浩等,2022)。由于远离南侧的雅鲁藏布缝合带,西藏中部受新特提斯洋俯冲以及印度—欧亚板块碰撞的影响相对较弱,新生代岩浆活动出露规模较小。近年来,在西藏中部陆续报道了始新世岩浆岩资料,这些岩浆岩多为壳源成因的中酸性火山岩,主要为区域上广泛分布的美苏组火山岩($E_{1-2}m$),最新的测年结果显示其形成时代与南侧始新世岩浆爆发的时间相一致(魏永峰等, 2018; 张耀玲等, 2018)。

本文研究区位于聂尔错以东约20 km(图1),大地构造位置处于北拉萨地块之上,区内地层以侏罗系木嘎岗日岩群(JM)、上侏罗统—下白垩统沙木罗组($J_3K_1s$)以及下白垩统郎山组($K_1l$)和多尼组($K_1d$)为主,规模巨大的早白垩世盐湖花岗岩体出露于研究区北部。在研究区中部的侏罗系—白垩系中沿构造裂隙发育着大量的中基性岩脉,然而这些岩脉的形成时代与成因不明,缺乏年代学与地球化学数据约束。本次研究的辉绿岩脉侵位于沙木罗组($J_3K_1s$)砂岩之中,岩脉宽1 m左右,近东西向延伸达百米(图2a),岩石呈灰白色,块状构造(图2b),辉绿结构,岩石发生一定程度蚀变,矿物组成以辉石和基性斜长石为主,粒径一般0.5 mm左右,次要矿物见少量角闪石和黑云母等,副矿物有磁铁矿和磷灰石等(图2c)。

## 3 测试方法与结果

本次共采集1件年代学和4件地球化学样品进行年代学与全岩地球化学分析研究。LA-ICP-MS锆石U-Pb同位素测定在吉林大学东北亚矿产资源

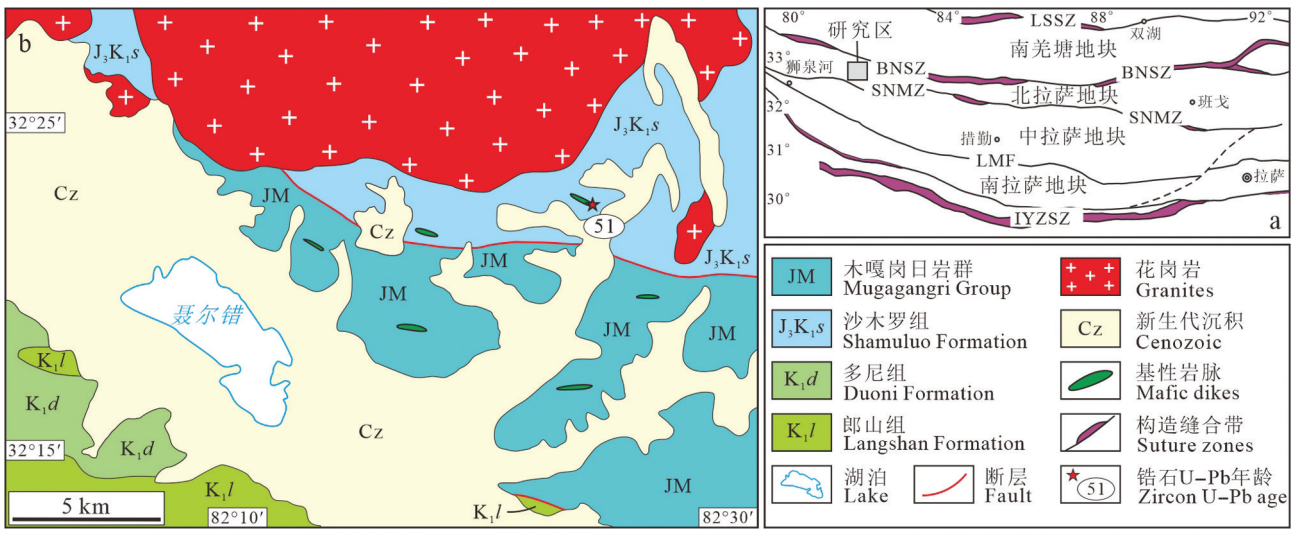


图1 青藏高原南部构造单元划分图(a)和聂尔错地区地质简图及采样位置(b)

LSSZ—龙木错—双湖缝合带;BNSZ—班公湖—怒江缝合带;SNMZ—狮泉河—纳木错混杂岩带;LMF—洛巴堆—米拉山断裂带;IYZSZ—雅鲁藏布缝合带

Fig.1 Tectonic subdivision of the southern Tibetan Plateau (a) and simplified geological map of the Nie'erco area and samples location (b)

LSSZ-Longmuco-Shuanghu suture zone; BNSZ-Bangonghu-Nujiang suture zone; SNMZ-Shiquan River-Namsto melange zone; LMF-Luobadui-Milashan Fault; IYZSZ-Indus-Yarlung Zangbo River suture zone


图2 聂尔错辉绿岩野外露头及镜下照片
Amp—角闪石;Px—辉石
Fig.2 Field and petrographic photographs of Nie'erco diabase
Amp-Amphibole; Px-Pyroxene

评价国土资源部重点实验室利用Agilent 7900型ICP-MS仪器完成,测试结果见表1。全岩主微量元素含量在武汉上谱分析科技有限责任公司完成,测试结果见表2。主量元素含量利用日本理学Primus Ⅱ X射线荧光光谱仪(XRF)分析完成,微量元素含量利用Agilent 7700e ICP-MS分析完成。

### 3.1 锆石U-Pb年龄

辉绿岩锆石整体呈无色透明的短柱或长柱状,晶形完好,粒径100~200 μm,长宽比在2∶1左右(图3)。本次共对17颗锆石进行测试分析工作,除去4颗99 Ma、101 Ma、115 Ma和180 Ma的古老捕获锆石外,13颗年轻锆石测点$^{206}Pb/^{238}U$年龄集中在50~52 Ma,在谐和图上(图3)所有测点都落在谐和线上或其附近区域,获得13颗年轻锆石$^{206}Pb/^{238}U$年龄加权平均值为(50.8±0.6)Ma(MSWD=0.64),此年龄代表了辉绿岩的形成时代。

### 3.2 全岩地球化学

辉绿岩样品整体具有低的$SiO_2$(51.1%~54.6%),高的全碱($Na_2O+K_2O$=5.93%~6.86%)、MgO(3.64%~4.46%)、$Al_2O_3$(16.9%~17.3%)和$TiO_2$(1.14%~1.49%)含量。在岩石分类Nb/Y-Zr/$TiO_2$图解中(图4),大部分辉绿岩样品落在碱性玄武岩区域。

**表1 聂尔错辉绿岩LA-ICP-MS锆石U-Pb定年结果**
**Table 1 LA-ICP-MS zircon U-Pb dating results of Nie'erco diabases**

| 测点 | 同位素比值 | | | | | | 年龄/Ma | | | | | |
|---|---|---|---|---|---|---|---|---|---|---|---|---|
| | $^{207}Pb/^{206}Pb$ | 1σ | $^{207}Pb/^{235}U$ | 1σ | $^{206}Pb/^{238}U$ | 1σ | $^{207}Pb/^{206}Pb$ | 1σ | $^{207}Pb/^{235}U$ | 1σ | $^{206}Pb/^{238}U$ | 1σ |
| 1 | 0.04621 | 0.00222 | 0.05071 | 0.00252 | 0.00796 | 0.00022 | 9 | 57 | 50 | 2 | 51 | 1 |
| 2 | 0.05017 | 0.00268 | 0.05401 | 0.00296 | 0.00781 | 0.00021 | 203 | 78 | 53 | 3 | 50 | 1 |
| 3 | 0.04733 | 0.00407 | 0.05213 | 0.00446 | 0.00799 | 0.00025 | 66 | 130 | 52 | 4 | 51 | 2 |
| 4 | 0.05003 | 0.00326 | 0.1237 | 0.0082 | 0.01793 | 0.00050 | 196 | 101 | 118 | 7 | 115 | 3 |
| 5 | 0.04716 | 0.00229 | 0.05231 | 0.00258 | 0.00804 | 0.00023 | 57 | 59 | 52 | 2 | 52 | 1 |
| 6 | 0.05002 | 0.00307 | 0.05383 | 0.00334 | 0.00781 | 0.00022 | 196 | 92 | 53 | 3 | 50 | 1 |
| 7 | 0.04605 | 0.00199 | 0.04922 | 0.00159 | 0.00775 | 0.00022 | | 92 | 49 | 2 | 50 | 1 |
| 8 | 0.04920 | 0.00151 | 0.1053 | 0.0036 | 0.01552 | 0.00040 | 157 | 37 | 102 | 3 | 99 | 3 |
| 9 | 0.04669 | 0.00551 | 0.05161 | 0.00609 | 0.00802 | 0.00023 | 33 | 204 | 51 | 6 | 51 | 1 |
| 10 | 0.04729 | 0.00191 | 0.05188 | 0.00218 | 0.00796 | 0.00021 | 64 | 50 | 51 | 2 | 51 | 1 |
| 11 | 0.04893 | 0.00228 | 0.1062 | 0.0051 | 0.01574 | 0.00041 | 144 | 66 | 102 | 5 | 101 | 3 |
| 12 | 0.05872 | 0.00350 | 0.06437 | 0.00390 | 0.00795 | 0.00022 | 557 | 84 | 63 | 4 | 51 | 1 |
| 13 | 0.05380 | 0.00520 | 0.05791 | 0.00559 | 0.00781 | 0.00023 | 363 | 165 | 57 | 5 | 50 | 1 |
| 14 | 0.04874 | 0.00223 | 0.05275 | 0.00251 | 0.00785 | 0.00021 | 135 | 63 | 52 | 2 | 50 | 1 |
| 15 | 0.04704 | 0.00219 | 0.05238 | 0.00252 | 0.00808 | 0.00022 | 51 | 59 | 52 | 2 | 52 | 1 |
| 16 | 0.04823 | 0.00221 | 0.05399 | 0.00256 | 0.00812 | 0.00022 | 111 | 62 | 53 | 2 | 52 | 1 |
| 17 | 0.05132 | 0.00112 | 0.2008 | 0.0054 | 0.02838 | 0.00072 | 255 | 28 | 186 | 5 | 180 | 5 |

表2 聂尔错辉绿岩主量元素(%)和微量元素($10^{-6}$)分析结果

Table 2 Analytical results of major (%) and trace elements($10^{-6}$) of Nie'erco diabases

| | T16h1 | T16h2 | T16h3 | T16h4 | | T16h1 | T16h2 | T16h3 | T16h4 |
|---|---|---|---|---|---|---|---|---|---|
| $SiO_2$ | 51.1 | 54.6 | 51.3 | 51.3 | Zr | 229 | 199 | 224 | 224 |
| $TiO_2$ | 1.49 | 1.14 | 1.42 | 1.46 | Nb | 23.0 | 14.6 | 22.4 | 22.5 |
| $Al_2O_3$ | 17.3 | 17.3 | 16.9 | 17.1 | Sn | 1.67 | 2.00 | 1.59 | 1.64 |
| $Fe_2O_3T$ | 8.91 | 8.91 | 8.34 | 8.82 | Cs | 3.12 | 3.32 | 2.33 | 2.76 |
| MnO | 0.13 | 0.16 | 0.13 | 0.13 | Ba | 765 | 415 | 540 | 713 |
| MgO | 4.46 | 3.64 | 4.10 | 4.31 | La | 46.7 | 33.8 | 45.1 | 46.4 |
| CaO | 5.41 | 6.15 | 6.40 | 5.62 | Ce | 95.7 | 66.4 | 93.8 | 96.3 |
| $Na_2O$ | 3.58 | 4.00 | 3.77 | 3.66 | Pr | 11.2 | 7.51 | 11.1 | 11.2 |
| $K_2O$ | 3.28 | 1.93 | 2.63 | 3.06 | Nd | 43.9 | 29.0 | 43.4 | 44.1 |
| $P_2O_5$ | 0.62 | 0.41 | 0.57 | 0.61 | Sm | 7.44 | 5.81 | 7.45 | 7.63 |
| LOI | 3.37 | 1.87 | 3.90 | 3.73 | Eu | 2.02 | 1.46 | 2.01 | 2.06 |
| Total | 99.6 | 100.1 | 99.5 | 99.7 | Gd | 5.78 | 4.93 | 5.59 | 5.91 |
| Li | 63.2 | 71.1 | 55.3 | 61.4 | Tb | 0.80 | 0.71 | 0.81 | 0.86 |
| Be | 1.72 | 1.45 | 1.65 | 2.00 | Dy | 4.53 | 3.95 | 4.54 | 4.57 |
| Sc | 17.3 | 18.2 | 16.2 | 16.9 | Ho | 0.90 | 0.86 | 0.86 | 0.89 |
| V | 186 | 192 | 177 | 178 | Er | 2.34 | 2.21 | 2.28 | 2.43 |
| Cr | 41.6 | 24.0 | 40.3 | 40.8 | Tm | 0.34 | 0.33 | 0.31 | 0.34 |
| Co | 24.4 | 18.7 | 24.5 | 23.9 | Yb | 2.05 | 2.04 | 1.89 | 1.98 |
| Ni | 41.6 | 25.8 | 41.2 | 40.7 | Lu | 0.32 | 0.36 | 0.33 | 0.32 |
| Cu | 30.5 | 5.2 | 73.8 | 15.5 | Hf | 5.39 | 4.57 | 5.20 | 5.38 |
| Zn | 87.3 | 145.7 | 80.2 | 86.8 | Ta | 1.26 | 0.82 | 1.17 | 1.22 |
| Ga | 21.0 | 21.1 | 21.7 | 21.1 | Tl | 0.82 | 0.57 | 0.61 | 0.73 |
| Rb | 136 | 98.4 | 105 | 126 | Pb | 6.87 | 60.71 | 8.18 | 7.04 |
| Sr | 726 | 545 | 779 | 727 | Th | 7.20 | 4.37 | 7.33 | 7.21 |
| Y | 23.9 | 22.7 | 23.2 | 23.9 | U | 1.17 | 1.10 | 1.16 | 1.21 |

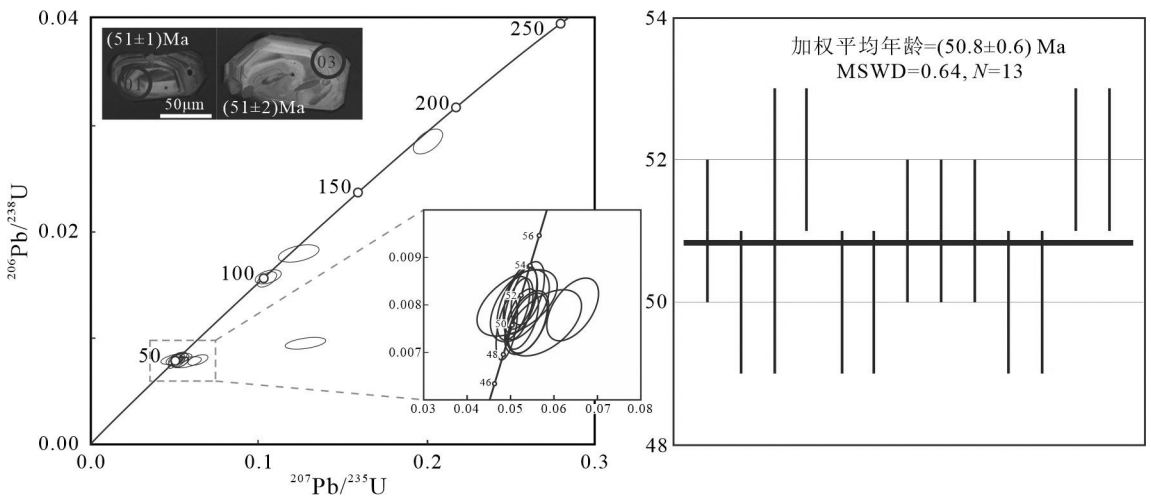


图3 辉绿岩锆石U−Pb谐和图

Fig.3 Zircon U−Pb concordia diagrams of diabase

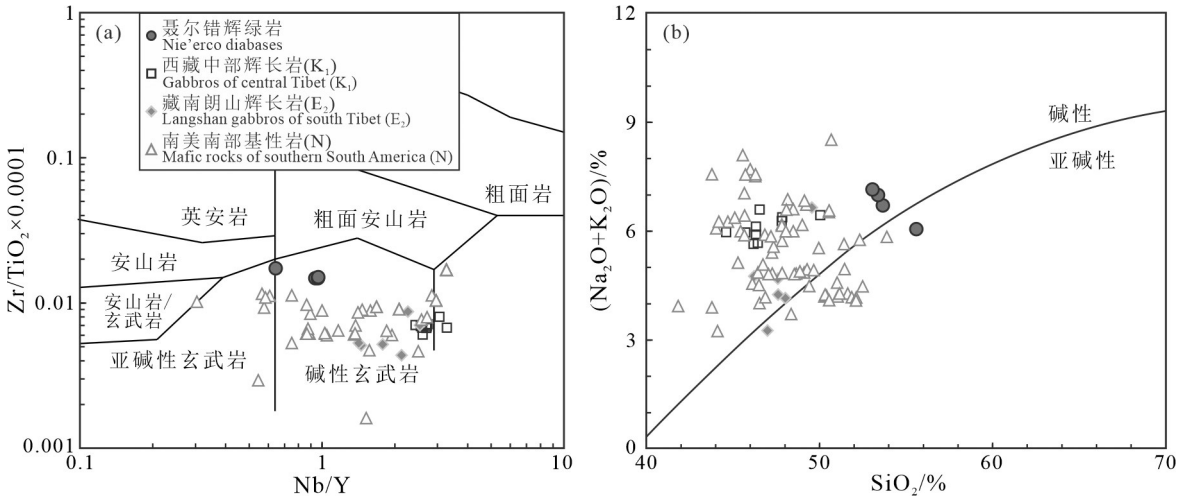


图4 Nb/Y−Zr/$TiO_2$图解(a,据Pearce, 1996)和$SiO_2$−($Na_2O$+$K_2O$)图解(b)(数据引自D'Orazio et al., 2001; Gorring et al., 2003; Espinoza et al., 2005; Ji et al., 2016; Wu et al., 2019a)

Fig.4 Nb/Y−Zr/$TiO_2$ diagram (a, after Pearce, 1996) and $SiO_2$−($Na_2O$+$K_2O$) diagram (b) (Data is from D'Orazio et al., 2001; Gorring et al., 2003; Espinoza et al., 2005; Ji et al., 2016; Wu et al., 2019a)

在球粒陨石标准化稀土元素配分曲线中,辉绿岩样品呈富集轻稀土元素、亏损重稀土元素的右倾模式($(La/Yb)_N$=12~17),Eu负异常不明显($\delta$Eu=0.83~0.95)(图5a)。在原始地幔标准化微量元素蛛网图中(图5b),辉绿岩样品显示Rb、Ba等大离子亲石元素(LILEs)的富集以及Nb、Ta等高场强元素(HFSEs)的亏损。

## 4 讨　论

### 4.1 岩石成因

辉绿岩样品具有低硅、富铁、镁、钙的主量元素含量以及高铬、镍等微量元素含量,显示幔源岩浆岩的地球化学特征,幔源岩浆在上升侵位及岩浆房内演化的过程中会受到地壳物质的混染作用(Castillo et al., 1999),因此地壳混染是探讨辉绿岩岩石成因不可回避的问题。锆石中古老捕获锆石的出现指示岩浆在上升过程中受到围岩物质的混染。此外,地壳组分通常具有低的MgO含量、高La/Nb、Th/Nb比值以及明显的Nb、Ta亏损(Rudnick and Fountain, 1995),因此地壳混染过程往往会导致原始岩浆成分向地壳端元演化,在$(La/Nb)_N$−$(Th/Nb)_N$和Nb/U−Nd/Pb图解中(图6),辉绿岩均表现出

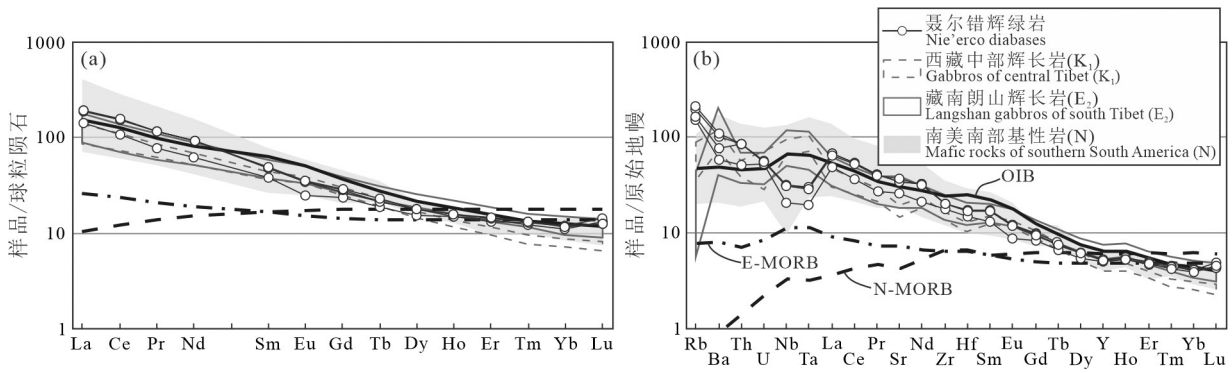


图5 球粒陨石标准化稀土元素模式图(a)和原始地幔标准化微量元素蛛网图(b)(OIB、E−MORB、N−MORB的平均值与微量元素的标准化值引自Sun and McDonough(1989),其他数据引用同图4)

OIB—洋岛玄武岩;N−MORB—亏损型洋中脊玄武岩;E−MORB—富集型洋中脊玄武岩

Fig.5 Chondrite−normalized rare earth element patterns (a) and primitive mantle−normalized trace element spider diagrams (b) (the average of OIB, E−MORB, N−MORB and normalized values of REE and trace elements are from Sun and McDonough (1989), other cited data is the same as Fig.4)

OIB−Oceanic island basalt; N−MORB−Normal mid−ocean ridge basalt; E−MORB−Enriched mid−ocean ridge basalt

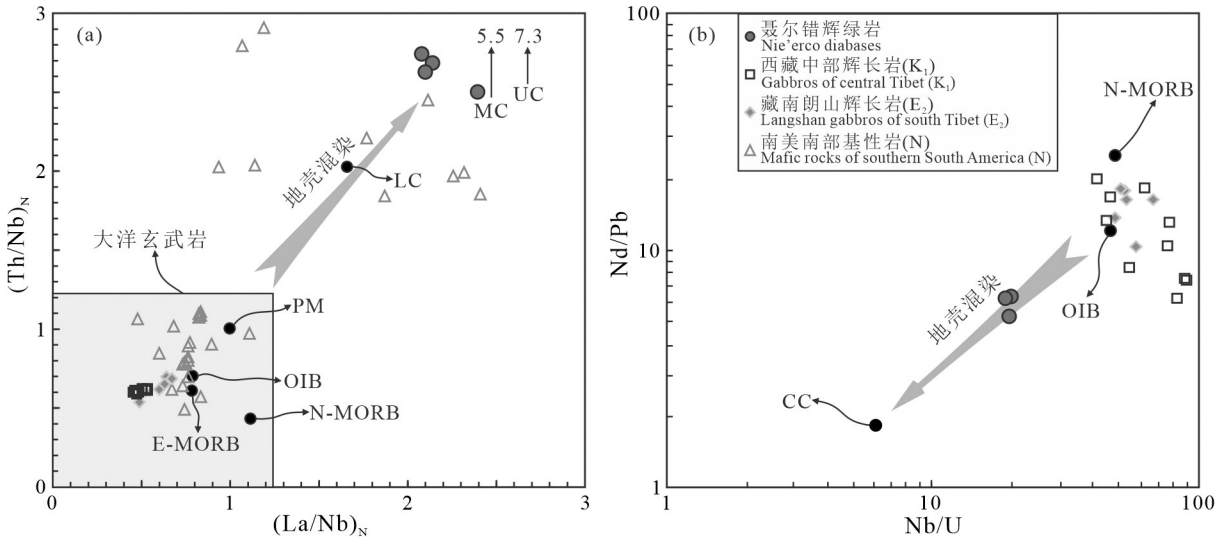


图6 $(La/Nb)_N$−$(Th/Nb)_N$图解(a, 据Frey et al., 2002)和Nb/U−Nd/Pb图解(b, 据Ji et al., 2016)(引用数据同图4)

PM—原始地幔;OIB—洋岛玄武岩;N−MORB—亏损型洋中脊玄武岩;E−MORB—富集型洋中脊玄武岩;LC—下地壳;MC—中地壳;UC—上地壳;CC—大陆地壳

Fig.6 $(La/Nb)_N$−$(Th/Nb)_N$ diagram (a, after Frey et al., 2002) and Nb/U−Nd/Pb diagram (b, after Ji et al., 2016) (the cited data is the same as Fig.4)

PM−Primitive Mantle; OIB−Oceanic island basalt; N−MORB−Normal mid−ocean ridge basalt; E−MORB−Enriched mid−ocean ridge basalt; LC−Lower crust; MC−Middle crust; UC−Upper crust; CC−Continental crust

地壳成分参与成岩的特征,地壳混染也合理解释了辉长岩样品中明显的Nb、Ta亏损(Rudnick and Gao, 2003)。因此,地球化学特征指示聂尔错辉绿岩在侵位过程中应该经历了一定程度的地壳混染作用。

聂尔错辉绿岩具有明显的轻重稀土分异特征,显示OIB型岩石的地球化学亲缘性。在Ti−V图解中(图7a),辉绿岩样品显示与典型OIB型岩石相似

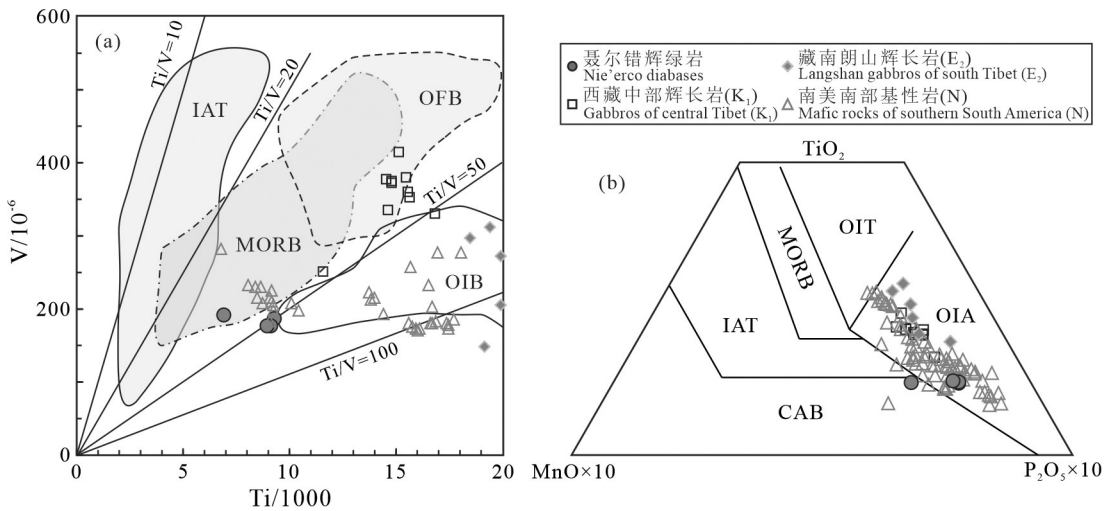


图7 Ti−V图解(a, 据Shervais, 1982)和$TiO_2$−MnO−$P_2O_5$图解(b, 据Mullen, 1983)(引用数据同图4)

IAT—岛弧拉斑玄武岩;MORB—洋中脊玄武岩;OFB—大洋溢流玄武岩;OIB—洋岛玄武岩;OIT—洋岛拉斑玄武岩;OIA—洋岛碱性玄武岩;CAB—钙碱性玄武岩

Fig.7 Ti−V diagram (a, after Shervais, 1982) and $TiO_2$−MnO−$P_2O_5$ diagram (b, after Mullen, 1983) (the cited data is the same as Fig.4)

IAT−Island arc tholeiite; MORB—Mid−ocean ridge basalt; OFB—Oceanic flood basalt; OIB—Oceanic island basalt; OIT—Oceanic island tholeiite; OIA—Oceanic island alkali basalt; CAB—Calc−alkaline basalt

的特征;在$TiO_2$-MnO-$P_2O_5$图解中(图7b),辉绿岩样品同样落在洋岛碱性玄武岩区域。碱性洋岛型岩石通常起源与相对富集的地幔源区,是深部软流圈地幔上涌熔融的产物(Ferrari et al., 2001; Gorring et al., 2003; Sklyarov et al., 2003; Wu et al., 2019a)。近年来,西藏南部陆续报道了大量的始新世基性岩浆作用,这些基性岩石同样具有OIB型的地球化学特征,研究认为起源于深部的软流圈地幔(Ji et al., 2016)。因此,本文认为聂尔错辉绿岩同样是深部软流圈地幔部分熔融的产物。

### 4.2 构造背景

青藏高原岩浆岩广泛发育,其时空展布具有明显的规律性,是深部动力学过程的重要岩石学记录(Chung et al., 2003, 2005; 莫宣学, 2011; Zhu et al., 2011)。研究区位于西藏中部的北拉萨地块之上,区域上岩浆活动以早白垩世晚期—晚白垩世为主,其深部构造演化主要受到班公湖—怒江洋俯冲消减以及拉萨—羌塘陆陆碰撞过程的影响(Zhu et al., 2011, 2016; Pan et al., 2012; Wu et al., 2018, 2019a, b; Liu et al., 2019),大量的研究资料支持班公湖—怒江洋在早白垩世早期已经消亡(Kapp et al., 2007; Raterman et al., 2014; Ma et al., 2017; Li et al., 2018),而早白垩世晚期—晚白垩世大规模的岩浆爆发应该形成于碰撞后伸展背景,其深部动力学机制与洋盆闭合后的板片断离与增厚岩石圈拆沉相关(Zhu et al., 2011, 2016; Wu et al., 2018, 2019a, b)。在晚白垩世之后区域岩浆活动减弱,拉萨地块与羌塘板块拼合成为一体,西藏中部进入板内演化阶段。在Zr-Zr/Y图解和Nb-Zr-Y图解中(图8),聂尔错辉绿岩样品均落在板内玄武岩区域,进一步表明西藏中部在始新世处于相对稳定的板内环境。

### 4.3 地球动力学机制

新特提斯洋构造演化史的研究一直是国内外学者关注的热点,其中印度-欧亚大陆的陆陆碰撞时限是众多学者关注的热点问题(Garzanti et al., 1987; Dewey et al., 1989; Yin and Harrison, 2000; Hu et al., 2016)。大量的年代学数据指示拉萨地块南缘在始新世早期(约50 Ma)存在大规模的岩浆爆发活动,其岩石地球化学特征以中酸性钙碱性岩石为主(孟元库等, 2015, 2018),早期的研究提出该期岩浆作用是新特提斯洋北向俯冲引发的弧形岩浆作用(Schärer et al., 1984; Searle et al., 1987),而近年来综合不同学科的研究资料揭示始新世早期岩浆爆发应该是印度—欧亚板块陆陆碰撞过程的产物

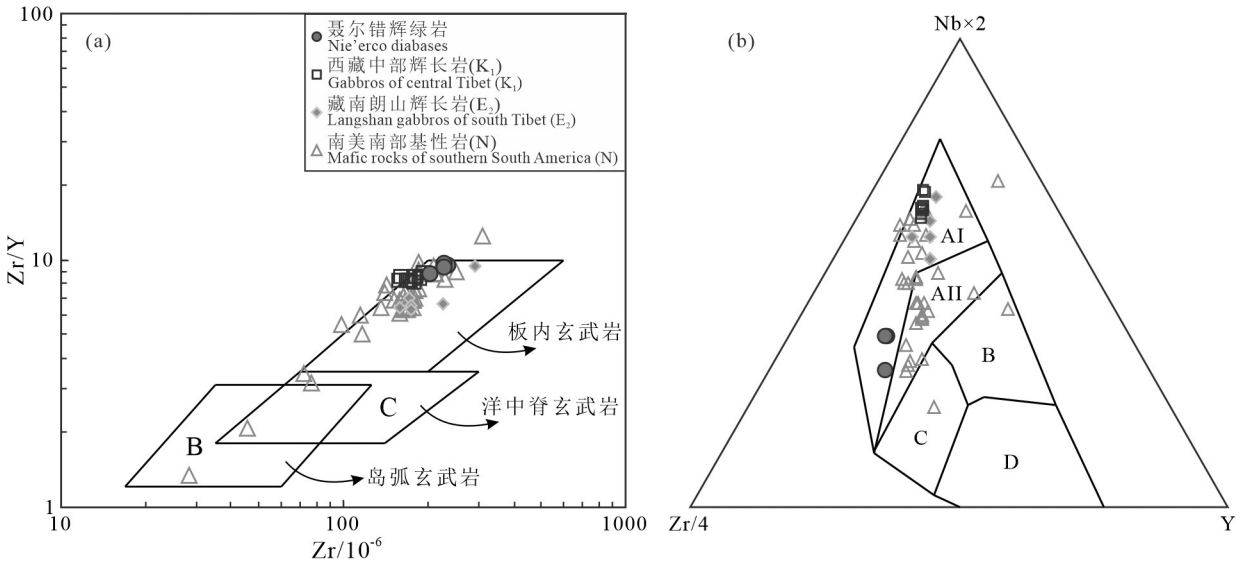


图8 Zr-Zr/Y图解(a, 据Pearce and Norry, 1979)和Nb×2-Zr/4-Y图解(b, 据Meschede, 1986)(引用数据同图4)

AI—板内碱性玄武岩;AII—板内碱性和拉斑玄武岩;B—富集型洋中脊玄武岩;C—板内拉斑和弧型玄武岩;D—亏损型洋中脊玄武岩和弧型玄武岩

Fig.8 Zr-Zr/Y diagram (a, after Pearce and Norry, 1979) and Nb×2-Zr/4-Y diagram (b, after Meschede, 1986) (the cited data is the same as Fig.4)

AI-Within-plate basalt; AII-Within-plate alkaline and within-plate tholeiite; B-Enriched mid-ocean ridge basalt; C-Within-plate basalt and volcanic arc basalt; D-Normal mid-ocean ridge basalt and volcanic arc basalt

(Wen et al., 2008; Ji et al., 2009, 2016; 莫宣学, 2011; Zhu et al., 2015, 2018; 陈兰朴等, 2019)。

近年来, 众多学者在拉萨地块南缘识别了大量的基性岩浆活动(Dong et al., 2005; 岳亚慧和丁林, 2006; Ji et al., 2016; Huang et al., 2017; 王旭辉等, 2019), 测年结果显示这些基性岩浆作用同样形成于始新世早期(57~47 Ma), 地球化学特征显示OIB型岩石的亲缘性。OIB型岩石的形成通常与深部软流圈地幔上涌相关, 可以形成于地幔柱或者板片窗等构造背景(Hole et al., 1991; Ferrari et al., 2001; Hawkesworth and Schersten, 2007; Wu et al., 2019a), 考虑到始新世岩浆作用在西藏南部呈条带状展布, 而且在西藏中部零星出露, 这与地幔柱引发的岩浆岩展布形态并不相符。而在陆陆碰撞过程中, 俯冲板片的前缘发生断离以及增厚的岩石圈发生拆沉均会导致深部软流圈地幔上涌并发生减压熔融, 形成具有OIB型岩石(Ji et al., 2016; Wu et al., 2019a)。通常增厚岩石圈拆沉会伴随着大规模的埃达克质岩浆爆发, 而大量的岩浆岩年代学与地球化学数据指示印度—欧亚板块碰撞形成的增厚岩石圈于渐新世发生拆沉(Chung et al., 2003, 2009)。大陆动力学研究提出在板块汇聚带陆陆碰撞过程中, 高密度的洋壳会拖曳低密度的陆壳进入地幔深度, 而二者之间的浮力差会导致洋壳最终会从陆壳边缘发生断离, 并在深部形成板片窗, 即板片断离过程(Davies and von Blanckenburg, 1995; van Hunen and Allen, 2011; Wu et al., 2016, 2019a)。板片窗的打开会直接导致深部软流圈地幔上涌, 同时诱导上覆岩石圈发生熔融, 形成平行于板块缝合带的带状岩浆活动, 这与拉萨地块南缘近东西向发育的始新世林子宗火山岩相一致(潘桂棠等, 2006; 莫宣学, 2011; 朱弟成等, 2017)。此外, 重力和远源地震数据指示印度大陆岩石圈边缘并不存在大洋岩石圈板片(Jin et al., 1996), 表明俯冲前缘洋壳已经从陆壳边缘发生断离(朱弟成等, 2017)。因此, 本文认为板片断离机制是拉萨地块上始新世岩浆活动最为合理的深部地球动力学解释(图9)。

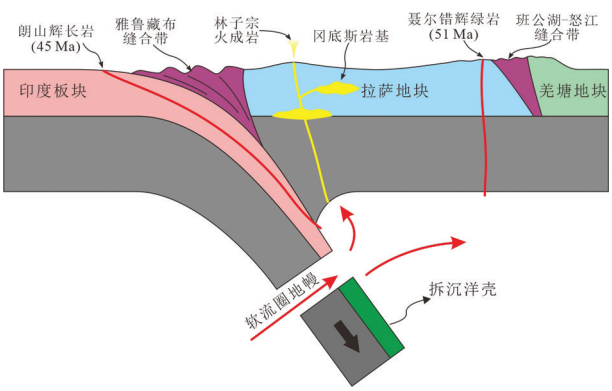


图9 青藏高原始新世构造-岩浆演化示意图
(修改自Ji et al., 2016)

Fig.9 Schematic illustration of the Eocene tectonic-magmatic evolution of the Tibetan Plateau
(modified from Ji et al., 2016)

尽管远离雅鲁藏布缝合带, 本次在北拉萨地块上新获得的辉绿岩资料表明印度—欧亚板块碰撞过程对西藏中部地区的构造-岩浆作用同样产生了一定的影响。最近, 在西南天山柯坪地区识别的萨尔干基性岩脉中同样获得了始新世早期的年龄信息((49.1±0.8) Ma), 其地球化学组成同样显示OIB型岩石的特征(霍海龙等, 2019)。这些远离俯冲带的OIB型岩石的识别表明新特提斯洋俯冲前缘洋壳在始新世早期板片断离之后, 深部软流圈地幔从板片窗快速上涌并逐渐向北运移, 不仅在拉萨地块南部形成了岩浆爆发事件, 同样在西藏中部乃至天山地区同样引发了一定程度的岩浆活动, 最终形成了在青藏高原上广泛发育的始新世岩浆岩。

## 5 结 论

(1)西藏中部聂尔错地区新识别的辉绿岩中获得了(50.8±0.6)Ma的锆石U-Pb谐和年龄, 与藏南地区始新世早期岩浆作用时代相一致。

(2)辉绿岩样品整体显示碱性OIB型岩石的地球化学特征, 是深部软流圈地幔上涌减压熔融的产物, 其深部动力学机制应该与南侧印度—欧亚板块碰撞后深俯冲的新特提斯洋洋壳板片断离过程相关。

(3)聂尔错地区始新世早期OIB型辉绿岩的识别, 结合近年来同时期岩浆作用的报道, 指示新特提斯洋板片断离过程对西藏中部构造-岩浆作用同样产生了重要的影响。

**致谢**: 野外调查与实验测试分析工作得到了吉林大学范建军博士、罗安波博士等的帮助, 3位审稿专家对论文提出的宝贵意见, 在此一并表示感谢。

## References


Castillo P R, Janney P E, Solidum R U. 1999. Petrology and geochemistry of Camiguin Island, southern Philippines: Insights to the source of adakites and other lavas in a complex arc setting[J]. Contributions to Mineralogy and Petrology, 134(1): 33−51.

Chen Lanpu, Huang Zesen, Jiang Badoji, Dawa Ziren, Taer Jie. 2019. Zircon U−Pb age and geochemical characteristics of igneous rocks from the Dianzhong Formation in the Shengong area of Tibet[J]. Geological Bulletin of China, 38(7): 1127−1135 (in Chinese with English abstract).

Chung S L, Lo, C H, Lee, T Y. 2003. Petrologic case for Eocene slab breakoff during the Indo− Asian collision: Comment[J]. Geology, 31: 7−8.

Chung S L, Chu M F, Zhang Y Q, Xie Y W, Lo C H, Lee T Y, Lan C Y, Li X H, Zhang Q, Wang Y Z. 2005. Tibetan tectonic evolution inferred from spatial and temporal variations in post− collisional magmatism[J]. Earth−Science Reviews, 68(3/4): 173−196.

Chung S, Chu M F, Ji J, Oreilly S Y, Pearson N J, Liu D, Lee T, Lo C. 2009. The nature and timing of crustal thickening in Southern Tibet: Geochemical and zircon Hf isotopic constraints from postcollisional adakites[J]. Tectonophysics, 477(1): 36−48.

Davies J H, von Blanckenburg F. 1995. Slab breakoff: A model of lithosphere detachment and its test in the magmatism and deformation of collisional orogens[J]. Earth and Planetary Science Letters, 129: 85−102.

Dewey J F, Cande S, Pitman W C. 1989. Tectonic evolution of the India−Eurasia collision zone[J]. Eclogae Geologicae Helvetiae, 82 (3): 717−734.

Dong G C, Mo X X, Zhao Z D, Wang L L, Chen T. 2005. Geochronologic constraints on the magmatic underplating of the Gangdise belt in the India−Eurasia collision: Evidence of SHRIMP II zircon U−Pb dating[J]. Acta Geologica Sinica (English Edition), 79: 787−794.

D'Orazio M, Agostini S, Innocenti F, Haller M J, Manetti P, Mazzarini F. 2001. Slab window− related magmatism from southernmost South America: The Late Miocene mafic volcanics from the Estancia Glencross Area (−52 S, Argentina−Chile)[J]. Lithos, 57(2/3): 67−89.

Espinoza F, Morata D, Pelleter E, Maury R C, Suárez M, Lagabrielle Y, Mireille Polvé M, Bellon H, Cotton J, la Cruzc R, Guivel C. 2005. Petrogenesis of the Eocene and Mio− Pliocene alkaline basaltic magmatism in Meseta Chile Chico, southern Patagonia, Chile: Evidence for the participation of two slab windows[J]. Lithos, 82(3): 315−343.

Ferrari L, Petrone C M, Francalanci L. 2001. Generation of oceanic− island basalt− type volcanism in the western Trans− Mexican volcanic belt by slab rollback, asthenosphere infiltration, and variable flux melting[J]. Geology, 29: 507−510.

Frey F A, Weis D, Borisova A Y U, Xu G. 2002. Involvement of continental crust in the formation of the Cretaceous Kerguelen Plateau: New perspectives from ODP Leg 120 sites[J]. Journal of Petrology, 43: 1207−1239.

Fu Wenchun, Kang Zhiqiang, Pan Huibin. 2014. Geochemistry, zircon U−Pb age and implications of the Linzizong Group volcanic rocks in Shiquan River area, western Gangdise belt, Tibet[J]. Geological Bulletin of China, 33(6): 850− 859 (in Chinese with English abstract).

Garzanti E, Baud A, Mascle G. 1987. Sedimentary record of the northward flight of India and its collision with Eurasia (Ladakh Himalaya, India)[J]. Geodinamica Acta (Paris), 1(4/5): 297−312.

Gorring M, Singer B, Gowers J, Kay S M. 2003. Plio− Pleistocene basalts from the Meseta del Lago Buenos Aires, Argentina: Evidence for asthenosphere− lithosphere interactions during slab window magmatism[J]. Chemical Geology, 193(3): 215−235.

Hawkesworth C, Schersten A. 2007. Mantle plumes and geochemistry[J]. Chemical Geology, 241: 319−331.

Hole M J, Rogers G, Saunders A D, Storey M. 1991. Relation between alkalic volcanism and slab− window formation[J]. Geology, 19(6): 657−660.

Hou Zengqian, Mo Xuanxue, Yang Zhiming, Wang Anjian, Pan Guitang, Qu Xiaoming, Nie Fengjun. 2006. Metallogeneses in the collisional orogen of the Qinghai− Tibet Plateau: Tectonic setting, tempo− spatial distribution and ore deposit types[J]. Geology in China, 33(2): 340−351 (in Chinese with English abstract).

Hu X, Garzanti E, Wang J, Huang W, An W, Webb A. 2016. The timing of India− Asia collision onset− Facts, theories, controversies[J]. Earth−Science Reviews, 160: 264−299.

Huang F, Xu J H, Zeng Y C, Chen J L, Wang B D, Yu H X, Chen L, Huang W L, Tan R Y. 2017. Slab breakoff of the Neo− Tethys Ocean in the Lhasa terrane inferred from contemporaneous melting of the mantle and crust[J]. Geochemistry, Geophysics, Geosystems, 18(11): 4074−4095.

Huo Hailong, Chen Zhengle, Chen Guimin, Zhang Qing, Han Fengbin, Zhang Wengan. 2019. The U−Pb geochronology and geochemical characteristics of the Saergan mafic rocks in the Keping area, southwest Tianshan, China[J]. Journal of Geomechanics, 25(S1): 60−65 (in Chinese with English abstract).

Ji W Q, Wu F Y, Chung S L, Li J X, Liu C Z. 2009. Zircon U−Pb geochronology and Hf isotopic constraints on petrogenesis of the Gangdese Batholith, southern Tibet[J]. Chemical Geology, 262: 229−245.

Ji W Q, Wu F Y, Chung S L, Wang X C, Liu C Z, Li Q L, Liu Z C, Liu X C, Wang J G. 2016. Eocene Neo− Tethyan slab breakoff constrained by 45 Ma oceanic island basalt− type magmatism in southern Tibet[J]. Geology, 44: 283−286.

Jin Y, McNutt M K, Zhu Y S. 1996. Mapping the descent of Indian and Eurasian plates beneath the Tibetan Plateau from gravity

anomalies[J]. Journal of Geophysical Research: Solid Earth, 101 (B5): 11275−11290.

Kapp P, DeCelles P G, Gehrels G E, Heizler M, Ding L. 2007. Geological records of the Lhasa− Qiangtang and Indo− Asian collisions in the Nima area of central Tibet[J]. Geological Society of America Bulletin, 119: 917−932.

Li S, Guilmette C, Yin C, Ding L, Zhang J, Wang H, Baral U. 2019. Timing and mechanism of Bangong− Nujiang ophiolite emplacement in the Gerze area of central Tibet[J]. Gondwana Research, 71: 179−193.

Liu Y, Wang M, Li C, Li S, Xie C, Zeng X, Dong Y, Liu J. 2019. Late Cretaceous tectono− magmatic activity in the Nize region, central Tibet: Evidence for lithospheric delamination beneath the Qiangtang−Lhasa collision zone[J]. International Geology Review, 61(5): 562−583.

Ma A, Hu X, Garzanti E, Han Z, Lai W. 2017. Sedimentary and tectonic evolution of the southern Qiangtang basin: Implications for the Lhasa− Qiangtang collision timing[J]. Journal of Geophysical Research: Solid Earth, 122(7): 4790−4813.

Meng Yuanku, Xu Zhiqin, Chen Xijie, Ma Xuanxu, He Zhenyu, Zhang Xuesong. 2015. Zircon geochronology and Hf isotopic composition of Eocene granite batholith from Xaitongmoin in Middle Gangdise and its geological significance[J]. Geotectonica et Metallogenia, 39 (5): 933−948 (in Chinese with English abstract).

Meng Yuanku, Xu Zhiqin, Gao Cunshan, Xu Yang, Li Rihui. 2018. The identification of the Eocene magmatism and tectonic significance in the middle Gangdese magmatic belt, southern Tibet[J]. Acta Petrologica Sinica, 34(3): 513− 546 (in Chinese with English abstract).

Meschede M. 1986. A method of discriminating between different types of mid−ocean ridge basalts and continental tholeiites with the Nb−Zr−Y diagram[J]. Chemical Geology, 56: 207−218.

Mo Xuanxue. 2011. Magmatism and evolution of the Tibetan Plateau[J]. Geological Journal of China Universities, 17(3): 351−367(in Chinese with English abstract).

Mullen E D. 1983. MnO− $TiO_2$− $P_2O_5$: A minor element discriminant for basaltic rocks of oceanic environments and its implications for petrogenesis[J]. Earth and Planetary Science Letters, 62: 53−62.

Pan Guitang, Mo Xuanxue, Hou Zengqian, Zhu Dacheng, Wang liquen, Li Guangming, Liao Zhongli. 2006. Spatial− temporal framework of the Gangdese Orogenic Belt and its evolution[J]. Acta Petrologica Sinica, 22(3): 521−533 (in Chinese with English abstract).

Pan G T, Wang L Q, Li R S, Yuan S H, Ji, W H, Yin F G, Zhang W P, Wang B D. 2012. Tectonic evolution of the Qinghai− Tibet Plateau[J]. Journal of Asian Earth Sciences, 53: 3−14.

Pearce J A, Norry M J. 1979. Petrogenetic implications of Ti, Zr, Y and Nb variations in volcanic rocks[J]. Contributions to Mineralogy and Petrology, 69: 33−47.

Pearce J A. 1996. A User's Guide to Basalt Discrimination Diagrams[C]//Wyman D A(ed.). Trace Element Geochemistry of Volcanic Rocks: Applications for Massive Sulphide Exploration, 12. Geological Association of Canada, Short Course Notes. 79−113.

Raterman N S, Robinson A C, Cowgill E S. 2014. Structure and detrital zircon geochronology of the Domar fold− thrust belt: Evidence of pre− Cenozoic crustal thickening of the western Tibetan Plateau[J]. Geological Society of America, Special Paper, 507: 89−114.

Ren Jishun, Zhao Lei, Li Chong, Zhu Junbin, Xiao Liwei. 2017. Thinking on Chinese tectonics——Duty and responsibility of Chinese geologists[J]. Geology in China, 44(1): 33−43 (in Chinese with English abstract).

Rudnick R L, Fountain D M. 1995. Nature and composition of the continental crust: A lower crustal perspective[J]. Reviews of Geophysics, 33(3): 267−309.

Rudnick R L, Gao S. 2003. Composition of the continental crust[J]. Treatise on Geochemistry, 3: 1−64.

Schärer U, Xu R H, Allègre C J. 1984. U− Pb geochronology of Gangdese (Transhimalaya) plutonism in the Lhasa−Xigaze region, Tibet[J]. Earth and Planetary Science Letters, 69(2): 311−320.

Searle M P, Windley B F, Coward M P, Cooper D J W, Rex A J, Rex D, Kumar S. 1987. The closing of Tethys and the tectonics of the Himalaya[J]. Geological Society of America Bulletin, 98(6): 678−701.

Shervais J. 1982. Ti− V plots and the petrogenesis of modern and ophiolitic lavas[J]. Earth and Planetary Science Letters, 59: 101−118.

Sklyarov E V, Gladkochub D P, Mazukabzov A M, Menshagin Y V, Pisarevsky S A. 2003. Neoproterozoic mafic dike swarms of the sharyzhalgai metamorphic massif, southern Siberian craton[J]. Precambrian Research, 122(1): 359−376.

Sun S S, McDonough W F. 1989. Chemical and isotopic systematics of oceanic basalts: Implications for mantle compositions and processes[J]. Geological Society, London, Special Publications, 42: 313−345.

van Hunen J, Allen M B. 2011. Continental collision and slab break− off: A comparison of 3− D numerical models with observations[J]. Earth and Planetary Science Letters, 302: 27−37.

Wang Bin, Xie Chaoming, Dong Yongsheng, Song Yuhang, Duan Menglong. 2022. Geochemical characteristics of ultramafic rocks in Sumdo area, Tibet and its enlightenment for the evolution of the Sumdo Paleo− Tethys Ocean[J]. Geological Bulletin of China, 41 (7): 1144−1154 (in Chinese with English abstract).

Wang Xuhui, Lang Xinghai, Deng Yulin, Xie Fuwei, Lou Yuming, Zhang He, Yang Zongyao. 2019. Eocene diabase dikes in the Tangbai area, southern margin of Lhasa terrane, Tibet: Evidence for the slab break−off of the Neo−Tethys Ocean[J]. Geology in China, 46(6): 1336−1355 (in Chinese with English abstract).

Wei Yongfeng, Xiao Yuanfu, Luo Wei, Deng Zejin, Zhao Zhiqiang, Lin Meiying. 2018. The chronology, geochemistry and geological significance of Early Eocene A- type granite in Zhagaerlejian, Gaize, Tibet[J]. Xinjiang Geology, 36(1): 51-59 (in Chinese with English abstract).

Wen D R, Liu D Y, Chung S L, Chu M F, Ji J Q, Zhang Q, Song B, Lee T Y, Yeh M W, Lo C H. 2008. Zircon SHRIMP U-Pb ages of the Gangdese Batholith and implications for Neo-tethyan subduction in southern Tibet[J]. Chemical Geology, 252(3/4): 191-201.

Wu H, Li C, Chen J W, Xie C M. 2016. Late Triassic tectonic framework and evolution of central Qiangtang, Tibet, SW China[J]. Lithosphere, 8: 141-149.

Wu H, Qiangba Z, Li C, Wang Q, Gesang W, Ciren O, Basang D. 2018. Geochronology and geochemistry of Early Cretaceous granitic rocks in the Dongqiao area, Central Tibet: Implications for magmatic origin and geological evolution[J]. The Journal of Geology, 126(2): 249-260.

Wu H, Sun S L, Liu H Y, Chu H, Ding W. 2019a. An Early Cretaceous slab window beneath central Tibet, SW China: Evidence from OIB-like alkaline gabbro in the Duolong area[J]. Terra Nova, 31 (1): 67-75.

Wu H, Chen J W, Wang Q, Yu Y P. 2019b. Spatial and temporal variations in the geochemistry of Cretaceous high-Sr/Y rocks in central Tibet[J]. American Journal of Science, 319(2): 105-121.

Wu Hao, Lin Zhaoxu, Jiang Ziqi, Wang Chonghao, Zheng Xin, Yang Rui. 2022. Zircon U-Pb ages and geochemical characteristics of basalts in Zhongcang area, central Tibet: Constraints on the evolution of Shiquan River-Namu Co back-arc basin[J]. Geological Bulletin of China, 41(10): 1728-1739 (in Chinese with English abstract).

Xu Zhiqin, Yang Jingsui, Li Haibing, Ji Shaocheng, Zhang Zeming, Liu Yan. 2011. On the Tectonics of the India-Asia Collision[J]. Acta Geologica Sinica, 85(1): 1-33 (in Chinese with English abstract).

Xu Zhiqin, Yang jingsui, Hou Zengqian, Zhang Zeming, Zeng Lingsen, Li Haibing, Zhang Jianxin, Li Zhonghai, Ma Xuxuan. 2016. The progress in the study of continental dynamics of the Tibetan Plateau[J]. Geology in China, 43(1): 1-42 (in Chinese with English abstract).

Yin A, Harrison T M. 2000. Geologic evolution of the Himalayan-Tibetan orogen[J]. Annual Review of Earth and Planetary Sciences, 28: 211-280.

Yu Shimian, Ma Xudong, Hu Yanchun, Chen Wei, Liu Qingping, Song Yang, Tang Jüxing. 2022. Post-subdution evolution of the Northern Lhasa Terrane, Tibet: Constraints from geochemical anomalies, chronology and petrogeochemistry[J]. China Geology, 5: 84-95.

Yue Yahui, Ding Lin. 2006. $^{40}Ar/^{39}Ar$ Geochronology, geochemical characteristics and genesis of the Linzhuou basic dikes, Tibet[J]. Acta Petrologica Sinica, 22(4): 855-866 (in Chinese with English abstract).

Zhang Yaoling, Shen Yanxu, Wu Zhenhan, Zhao Zhen. 2018. Zircon U-Pb ages of magmatic rocks from Meisu formation in Gerze area in Tibet and its geological significance[J]. Journal of Geomechanics, 24(1): 128-136 (in Chinese with English abstract).

Zhao Yayun, Liu Xiaofeng, Yang Chunsi, Zhang Xiaoqiang, Liu Yuanchao, Zheng Changyun, Gong Fuzhi, Hua Kang. 2022. Recongnition of A-type granite and its implication for magmatism and mineralization in Tangge skarn-type Cu-polymetallic deposit, Tibet[J]. Geology in China, 49(2): 496-517 (in Chinese with English abstract).

Zhao Zhidan, Mo Xuanxue, Nomade S, Renne P R, Zhou Su, Dong Guocheng, Wang Liangliang, Zhu Dicheng, Liao Zhongli. 2006. Post-collisional ultrapotassic rocks in Lhasa Block, Tibetan Plateau: Spatial and temporal distribution and its implications[J]. Acta Petrologica Sinica, 22(4): 787-794 (in Chinese with English abstract).

Zhu D C, Zhao Z D, Niu Y, Mo X X, Chung S L, Hou Z Q. 2011. The Lhasa Terrane: Record of a microcontinent and its histories of drift and growth[J]. Earth and Planetary Science Letters, 301: 241-255.

Zhu D C, Wang Q, Zhao Z D, Chung S L, Cawood P A, Niu Y, Liu S A, Wu F Y, Mo X X. 2015. Magmatic record of India-Asia collision[J]. Scientific Reports, 5: 17236.

Zhu D C, Li S M, Cawood P A, Wang Q, Zhao Z D, Liu S A, Wang L Q. 2016. Assembly of the Lhasa and Qiangtang terranes in central Tibet by divergent double subduction[J]. Lithos, 245: 7-17.

Zhu D C, Wang Q, Chung S L, Cawood P A, Zhao Z D. 2018. Gangdese magmatism in southern Tibet and India-Asia convergence since 120 Ma[J]. Geological Society, London, Special Publications, 483: SP483.14.

Zhu Dicheng, Wang Qing, Zhao Zhidan. 2017. Constraining quantitatively the timing and process of continent-continent collision using magmatic record: Method and examples[J]. Science China (Earth Sciences), 47(6): 657-673 (in Chinese with English abstract).

## 附中文参考文献

陈兰朴, 黄泽森, 江巴多吉, 达瓦次仁, 塔尔杰. 2019. 西藏神公地区典中组火成岩锆石U-Pb年龄及地球化学特征[J]. 地质通报, 38 (7): 1127-1135.

付文春, 康志强, 潘会彬. 2014. 西藏冈底斯带西段狮泉河地区林子宗群火山岩地球化学特征、锆石U-Pb年龄及地质意义[J]. 地质通报, 33(6): 850-859.

侯增谦, 莫宣学, 杨志明, 王安建, 潘桂棠, 曲晓明, 聂凤军. 2006. 青藏高原碰撞造山带成矿作用：构造背景、时空分布和主要类型[J]. 中国地质, 33(2): 340-351.

霍海龙, 陈正乐, 陈贵民, 张青, 韩凤彬, 张文高. 2019. 西南天山柯坪地区萨尔干基性岩脉U-Pb年代学及地球化学特征[J]. 地质力学学报, 25(S1): 60-65.

孟元库, 许志琴, 陈希节, 马绪宣, 贺振宇, 张雪松. 2015. 藏南冈底斯中段谢通门始新世复式岩体锆石U−Pb年代学、Hf同位素特征及其地质意义[J]. 大地构造与成矿学, 39(5): 933−948.

孟元库, 许志琴, 高存山, 徐扬, 李日辉. 2018. 藏南冈底斯岩浆带中段始新世岩浆作用的厘定及其大地构造意义[J]. 岩石学报, 34(3): 513−546.

莫宣学. 2011. 岩浆作用与青藏高原演化[J]. 高校地质学报, 17(3): 351−367.

潘桂棠, 莫宣学, 侯增谦, 朱弟成, 王立全, 李光明, 廖忠礼. 2006. 冈底斯造山带的时空结构及演化[J]. 岩石学报, 22(3): 521−533.

任纪舜, 赵磊, 李崇, 朱俊宾, 肖黎微. 2017. 中国大地构造研究之思考——中国地质学家的责任与担当[J]. 中国地质, 44(1): 33−43.

王斌, 解超明, 董永胜, 宋宇航, 段梦龙. 2022. 西藏松多地区超基性岩地球化学特征及对松多古特提斯洋演化的启示[J]. 地质通报, 41(7): 1144−1154.

王旭辉, 郎兴海, 邓煜霖, 谢富伟, 娄渝明, 张赫, 杨宗耀. 2019. 西藏拉萨地体南缘汤白地区始新世辉绿岩脉——新特提斯洋壳断离的证据[J]. 中国地质, 46(6): 1336−1355.

魏永峰, 肖渊甫, 罗巍, 邓泽锦, 赵志强, 林美英. 2018. 西藏改则扎嘎尔勒尖早始新世A型花岗岩年代学、地球化学及地质意义[J]. 新疆地质, 36(1): 51−59.

吴浩, 林兆旭, 姜子崎, 王崇浩, 郑鑫, 仰睿. 2022. 西藏中部中仓地区玄武岩锆石U−Pb年龄与岩石地球化学特征: 对狮泉河-纳木错弧后洋盆演化的制约[J]. 地质通报, 41(10): 1728−1739.

许志琴, 杨经绥, 李海兵, 嵇少丞, 张泽明, 刘焰. 2011. 印度−亚洲碰撞大地构造[J]. 地质学报, 85(1): 1−33.

许志琴, 杨经绥, 侯增谦, 张泽明, 曾令森, 李海兵, 张建新, 李忠海, 马绪宣. 2016. 青藏高原大陆动力学研究若干进展[J]. 中国地质, 43(1): 1−42.

岳雅慧, 丁林. 2006. 西藏林周基性岩脉的$^{40}Ar/^{39}Ar$年代学、地球化学及其成因[J]. 岩石学报, 22(4): 855−866.

张耀玲, 沈燕绪, 吴珍汉, 赵珍. 2018. 西藏改则地区美苏组岩浆岩锆石U−Pb年龄及地质意义[J]. 地质力学学报, 24(1): 128−136.

赵亚云, 刘晓峰, 杨春四, 张小强, 刘远超, 郑常云, 龚福志, 华康. 2022. 西藏唐格矽卡岩型铜多金属矿床A型花岗岩的识别及其对成岩成矿的指示[J]. 中国地质, 49(2): 496−517.

赵志丹, 莫宣学, Nomade S, Renne P R, 周肃, 董国臣, 王亮亮, 朱弟成, 廖忠礼. 2006. 青藏高原拉萨地块碰撞后超钾质岩石的时空分布及其意义[J]. 岩石学报, 22(4): 787−794.

朱弟成, 王青, 赵志丹. 2017. 岩浆岩定量限定陆−陆碰撞时间和过程的方法和实例[J]. 中国科学:地球科学, 47(6): 657−673.